Journal of Intelligent & Robotic Systems (2024) 110:28
https://doi.org/10.1007/s10846-024-02060-z

REGULAR PAPER

Optimal Transport and Model Predictive Control-based Simultaneous Task Assignment and Trajectory Planning for Unmanned System Swarm

Xiwei Wu[1] · Bing Xiao[1] · Lu Cao[2] · Haibin Huang[3]

Received: 19 September 2023 / Accepted: 16 January 2024 / Published online: 3 February 2024

Abstract
This paper presents a simultaneous task assignment and trajectory planning method for unmanned system swarm by using optimal transport and model predictive control (OT-MPC). Unlike the conventional hierarchical assignment and planning, the proposed approach addresses both the task assignment and trajectory planning subproblems concurrently. To be specific, a unified cost function is designed to solve task assignment and trajectory planning problem. Moreover, the multi-tasks are assigned by using optimal transport, which establishes an optimal mapping between tasks and unmanned system vehicles based on transportation cost. The trajectory planning is achieved by using model predictive control, which generates high-quality navigation trajectories considering obstacle avoidance. Finally, the proposed method is applied to the unmanned surface vehicles swarm. Numerical simulations and experiments were conducted to validate the effectiveness of the proposed method.

Keywords Unmanned system swarm · Simultaneous task assignment and trajectory planning · Optimal transport · Model predictive control

1 Introduction

With the continuous advancement of environmental perception, information fusion, and control decision-making technologies, unmanned system swarm (USS) has rapidly evolved and found extensive applications in various fields, including military, rescue, and logistics [1, 2]. The unmanned system vehicles comprising the USS may be unmanned ground vehicles [3], unmanned aircraft vehicles [4], unmanned surface vehicles [5] or spacecraft [6, 7]. As application scenarios increase, the complexity of USS missions significantly grows. Hence, to ensure safe and effective execution of complex tasks, the task assignment and trajectory planning method for USS design has received more and more attention from the theoretical and engineering areas [8, 9].

In recent years, task assignment and trajectory planning methods for USS have been studied as different sub-problems. Substantial advancements have been achieved in the domain of multiple task assignment [10], with notable approaches including the Hungarian algorithm [11], particle swarm optimization (PSO) [12], self-organizing map [13, 14], and deep learning techniques [15, 16]. Meanwhile, several approaches have been proposed to address another sub-problem trajectory planning, such as genetic algorithm [17], PSO [18], A* algorithm [19], pseudospectral convex programming [20] and model predictive control [21, 22]. However, traditional methods often handle task assignment and trajectory planning as separate and independent sub-problems, overlooking their interdependencies. This can lead to sub-optimal or locally optimal solutions, failing to ensure global optimality or near-optimality of overall performance.

✉ Bing Xiao
xiaobing@nwpu.edu.cn

Xiwei Wu
wxw-treffen@mail.nwpu.edu.cn

Lu Cao
caolu_space2015@163.com

Haibin Huang
huanghaibin@hitwh.edu.cn

1 School of Automation, Northwestern Polytechnical University, Xi'an 710072, China

2 National Innovation Institute of Defense Technology, Chinese Academy of Military Science, Beijing 100071, China

3 School of Information Science and Engineering, Harbin Institute of Technology, Weihai 264209, China

To address the above weakness, the simultaneous task assignment and trajectory planning methods were presented [23–25]. This method simultaneously addresses two problems: assigning unmanned swarm individuals to target locations and generating collision-free trajectories for each individual. In [26, 27], a concurrent task assignment and trajectory planning method was presented, which minimize a cost function based on the square of velocity along the trajectory. However, this approach assumes that the convex hull of initial locations and desired task locations is obstacle-free. In [28], a method for solving chance-constrained simultaneous task assignment and path planning on a graph with stochastic edge costs was presented. In [29], the conflict graph is designed to simultaneously encode the traveling time cost of the subsequent path planning result of each task-robot assignment and address the predicted path conflicts of each two assignments. However, the focus of these methods is still on task assignment and ignores the effect of swarm individual dynamics on trajectories.

It is worth mentioning that the above methods lack randomness in the process of target assignment. Once the tasks are determined by the unmanned swarm individuals, the assignments will not be changed, which may lead to sub-optimal solutions. Additionally, excessive focus on task assignment neglects proper trajectory planning, resulting in non-continuous and non-smooth trajectories. Motivated by solving this problem, a simultaneous task assignment and trajectory planning method for USS by using OT-MPC is presented in this paper. The randomness of task assignment is enhanced by optimal transport theory through probabilistic transfers, and the collision probability among unmanned swarm individuals is reduced by trajectory prediction through model predictive control. The main contributions of this article are as follows:

1) A simultaneous task assignment and trajectory planning method for USS is presented. Both the task assignment and trajectory planning sub-problems are addressed concurrently. Comparing with [27, 28], a unified objective function is designed to facilitate the coordination and consistency between task assignment and trajectory planning. The risk of compromising overall performance is mitigated by avoiding local optimization.
2) The proposed method utilizes optimal transport and model predictive control to achieve simultaneous optimization of task assignment and trajectory planning, enabling rapid adjustments and re-planning in response to real-time information. Comparing with the existing simultaneous task assignment and trajectory planning such as [27, 29], the optimal transport method is utilized to match tasks randomly to unmanned system vehicles based on their costs, while the model predictive control is employed to iteratively optimize the trajectories of the unmanned system vehicles based on real-time feedback and predictions. The proposed approach is more applicable to the actual large-scale unmanned system swarm.
3) The Sinkhorn-Newton method is proposed, which is capable of rapidly obtaining the global optimal solution and demonstrates high efficiency and scalability for large-scale USS tasks. Hence, the proposed approach has greater application potential.

The paper is organized as follows: Some preliminaries and problem formulation are introduced in Section 2. In Section 3, OT-MPC method for simultaneous task assignment and trajectory planning is presented. The proposed method is applied to unmanned surface vehicle swarm in Section 4. The effectiveness of the proposed control approach is validated in Section 5. Some conclusions are given in Section 6 to end this work.

2 Preliminaries and Problem Formulation

Let $\mathbb{R}$ be the set of real numbers, and $\mathbb{R}^{m\times n}$ is the set of $m \times n$ real matrices. The vector $\mathbf{1}_m$ denotes an ones vector of dimension m, and $\boldsymbol{I}$ represents the identity matrix. The notation $[[N]]$ refers to the set $1, \ldots, N$. The Euclidean norm is represented by $||\cdot||$. For any $\boldsymbol{a} \in \mathbb{R}^{1\times n}$, a_i denotes its ith element and $diag(\boldsymbol{a})$ represents the diagonal matrix with its ith diagonal element being a_i, $i = 1, 2, \cdots, n$.

2.1 Monge Problem

In this subsection, the discrete optimal transport is given, and indicate how it relates to task assignment problem. Optimal transport is a mathematical theory and optimization approach utilized for computing the optimal mapping between two probability distributions [30, 31]. Consider two finite metric spaces, $\mathcal{X} \subset \mathbb{R}^m$ and $\mathcal{Y} \subset \mathbb{R}^n$. Let μ and ν be two discrete probability measures on $\mathcal{X}$ and $\mathcal{Y}$ respectively, satisfying the following conditions

$$\mu = \sum_{i\in m, a\in\mathcal{X}} \mu_{a_i}\delta_a,\ \nu = \sum_{j\in n, b\in\mathcal{Y}} \nu_{b_j}\delta_b \tag{1}$$

where μ_{a_i} and ν_{b_j} are the massed assigned to $a \in \mathcal{X}$ and $b \in \mathcal{Y}$. δ_a and δ_b are the Dirac delta at a and b, respectively.

Let $c : \mathcal{X} \times \mathcal{Y} \to \mathbb{R}$ be a cost function, where $c(a_i, b_j)$ denotes the transport cost from a_i in $\mathcal{X}$ to b_j in $\mathcal{Y}$, for every $1 \leqslant i \leqslant m$ and $1 \leqslant j \leqslant n$. The objective is to find a transport map $\mathcal{T} : \mathcal{X} \to \mathcal{Y}$ such that $\mathcal{T}_{\#}\mu = \nu$, meaning that the pushforward measure of μ under $\mathcal{T}$ is equal to ν. In other words, for each $j = 1, \dots, n$, one has $\nu_{b_j} = \sum_{\mathcal{T}(a_i)=b_j} \mu_{a_i}$. The goal is to minimize the total transport cost. Hence, the Monge Problem [32] can be formulated as follows

$$(M_P) = \min_{\mathcal{T}} \left\{ \sum_i c(a_i, \mathcal{T}(a_i)) : \mathcal{T}_{\#}\mu = \nu \right\} \tag{2}$$

Assume that $\mathcal{X}$ indicates the set of unmanned system vehicles, and $\mathcal{Y}$ denotes the set of tasks. Let $m = n = N$, and $\boldsymbol{\mu}_a = \boldsymbol{\nu}_b = \mathbf{1}_N/N$. N is the total number of unmanned system vehicles. The optimal map T determines the optimal task assignment, ensuring that each unmanned system vehicle a_i is assigned to a unique task b_j, establishing a one-to-one correspondence between the vehicles and the tasks.

2.2 Kantorovich Problem

The Monge problem mentioned above is a non-convex optimization problem that involves probability measures and transport costs. It cannot guarantee the existence of an optimal transport mapping from $(\mathcal{X}, \mu)$ to $(\mathcal{Y}, \nu)$. To address these limitations, Kantorovich introduced a more concise and efficient model for optimal transport by relaxing the requirement of fully deterministic transport. Kantorovich relaxes the Monge problem to a standard linear programming problem

$$(K_P) = \min_{\boldsymbol{P}\in\Pi(\boldsymbol{\mu}_a,\boldsymbol{\nu}_b)} \sum_{i,j} c(a_i, b_j) p_{ij} \tag{3}$$

where p_{ij} is the ith row and the jth column element of matrix $\boldsymbol{P}$, which indicates the amount of mass flowing from a_i towards b_j, $i = 1, 2, \dots, N$, $j = 1, 2, \dots, N$. Moreover, the matrix $\boldsymbol{P}$ has the following property

$$\Pi(\boldsymbol{\mu}_a, \boldsymbol{\nu}_b) := \{\boldsymbol{P} \in \mathbb{R}_+^{N\times N} : \boldsymbol{P}\mathbf{1}_N = \boldsymbol{\mu}_a, \boldsymbol{P}^{\mathrm{T}}\mathbf{1}_N = \boldsymbol{\nu}_b\} \tag{4}$$

2.3 Predictive Model of Unmanned System Swarm

In this paper, not only the one-to-one task assignment problem is considered, but also the problem of each swarm individual reaches the desired target with the optimal trajectory is studies. To address the latter problem, the MPC is employed to generate optimal trajectories, enabling efficient and real-time tracking.

Let $\boldsymbol{x}_i(k)$ indicate the state variables at time step k for the i-th unmanned system vehicle. The control input is denoted as $\boldsymbol{u}_i(k)$. Hence, the state space model for the i-th unmanned system vehicle is given by

$$\boldsymbol{x}_i(k+1) = f(\boldsymbol{x}_i(k), \boldsymbol{u}_i(k)), i = 1, \dots, N \tag{5}$$

where f represents a nonlinear continuous function.

By applying MPC, the prediction states of the i-th unmanned system vehicle is defined as follows

$$\boldsymbol{x}_i(k+p+1) = f(\boldsymbol{x}_i(k+p|k), \boldsymbol{u}_i(k+p|k)),\ p=0, \dots, N_h-1 \tag{6}$$

where $\boldsymbol{x}_i(k+p|k)$ denote the ith unmanned system vehicle's state at time step $k+p$, predicted at the time step k. The corresponding control actions are denoted by $\boldsymbol{u}_i(k+p|k)$. N_h is the predictive horizon.

2.4 Problem Formulation

The simultaneous task assignment and trajectory planning problem of this work can be stated as: Considering the unmanned system swarm's motion dynamics with state and control input constraints, given the initial position state $\{\boldsymbol{x}_i^0\}_{i=1}^N$ of the USS and the position of desired tasks $\{\boldsymbol{x}_j^d\}_{j=1}^N$, the objective is to find an optimal task assignment plan $\sigma : [\![N]\!] \to [\![N]\!]$ and control inputs $\{\boldsymbol{u}_i\}_{i=1}^N$ that solve the following optimization problem

$$\min_{\sigma} \sum_{i\in[\![N]\!]} c_{N_h}^i(\boldsymbol{x}_i^0, \boldsymbol{x}_{\sigma(i)}^d) \tag{7}$$

where the cost function $c_{N_h}^i$ is defined as

$$\begin{aligned}
&c_{N_h}^i(\boldsymbol{x}_i^0, \boldsymbol{x}_{\sigma(i)}^d) = \arg\min_{\boldsymbol{u}_i} \sum_{k=0}^{N_h-1} \mathcal{L}_i(\boldsymbol{x}_i(k), \boldsymbol{u}_i(k); \boldsymbol{x}_j^d)\\
&\text{subject to}\\
&\boldsymbol{x}_i(k+p+1) = f(\boldsymbol{x}_i(k+p|k), \boldsymbol{u}_i(k+p|k)),\\
&p = 0, \dots, N_h-1\\
&\boldsymbol{x}_i(k+p+1) \in \mathcal{W}_i, \boldsymbol{u}_i(k+p|k) \in \mathcal{U}_i\\
&\boldsymbol{x}_i[0] = \boldsymbol{x}_i^0
\end{aligned} \tag{8}$$

where $\mathcal{W}_i$ and $\mathcal{U}_i$ denote the state and control input constraints of the i-th unmanned system vehicle, respectively. $\mathcal{L}_i(\boldsymbol{x}_i(k), \boldsymbol{u}_i(k); \boldsymbol{x}_j^d)$ is the cost function of model predictive control.

Remark 1 A unified cost function Eq. (7) is designed to solve the problem of task assignment and trajectory planning simultaneously. Moreover, the task assignment problem is addressed by utilizing optimal transport Eqs. (3) and (4), while the trajectory planning is achieved by using model predictive control Eq. (8). Each solution of the cost function requires the mutual coordination of task assignment and path planning.

3 OT-MPC for Simultaneous Task Assignment and Trajectory Planning

According to Eqs. (7) and (8), the optimal task assignment and trajectory planning for the USS can be achieved when the optimal permutation σ^* and control inputs $\boldsymbol{u}^{MPC}(\boldsymbol{x}(k), \boldsymbol{x}^d_{\sigma^*})$ are determined. However, relying solely on the initial and target states to obtain the permutation may not yield an optimal task assignment. Additionally, with the increase of the swarm scale, the computational complexity of task assignment and trajectory planning also escalates. Hence, a temporary target state is introduced to solve the optimal permutation problem, and the Sinkhorn-Newton with MPC method is proposed to mitigate computational complexity.

3.1 Entropy Regularization for Optimal Transport

Entropy regularization can be utilized to find the approximate value to achieve fast solution for optimal transport. The Kantorovich problem Eq. (3) is rewritten by through the entropy regularization [33]

$$(K_P)^{\varepsilon} = \min_{\boldsymbol{P}\in\Pi(\boldsymbol{\mu}_a,\boldsymbol{\nu}_b)} \sum_{i,j} c(a_i, b_j) p_{ij} - \varepsilon H(\boldsymbol{P}) \tag{9}$$

where $H(\boldsymbol{P}) = -\sum_{i,j} p_{ij}(\log((p_{ij}) - 1)$ is the cost function of regularization, ε is regularization parameter.

For each permutation $\sigma \in [\![N]\!]$, the corresponding permutation matrix $\boldsymbol{P}_\sigma$ is defined as follows

$$p^{\sigma}_{ij} = \begin{cases} 1, if\ j = \sigma(i) \\ 0, otherwise \end{cases} \tag{10}$$

According to [33, 34], the temporary target state $\boldsymbol{x}^{temp}_i(\boldsymbol{P})$ is given by

$$\boldsymbol{x}^{temp}_i(\boldsymbol{P}) = N \sum_{j=1}^{N} p_{ij} \boldsymbol{x}^d_j \tag{11}$$

Note that for a permutation matrix $\boldsymbol{P}_\sigma$, it can be observed that $N\sum_{j=1}^{N} p^{\sigma}_{ij}\boldsymbol{x}^d_j = \boldsymbol{x}^d_{\sigma(i)}$.

Hence, with the temporary target state $\boldsymbol{x}^{temp}_i(\boldsymbol{P})$, the state of the USS at each moment is given by

$$\boldsymbol{x}_i(k+1) = f(\boldsymbol{x}_i(k), \boldsymbol{u}^{MPC}_i(\boldsymbol{x}_i(k), \boldsymbol{x}^{temp}_i(\boldsymbol{P}^*(\boldsymbol{x}(k))))) \tag{12}$$

$$\boldsymbol{P}^*(\boldsymbol{x}) = \min_{\boldsymbol{P}\in\Pi(\boldsymbol{1}_N/N,\boldsymbol{1}_N/N)} \sum_{i,j\in[\![N]\!]} \boldsymbol{c}^i_{N_h}(\boldsymbol{x}_i, \boldsymbol{x}^d_{\sigma(i)}) p_{ij} - \varepsilon H(\boldsymbol{P}) \tag{13}$$

where $\boldsymbol{x}(k) := [\boldsymbol{x}_1(k); \boldsymbol{x}_2(k); \cdots; \boldsymbol{x}_N(k)]$.

Remark 2 The solution of the cost function Eq. (7) is transformed into solving Eqs. (12) and (13). At each moment, the multi-task assignment problem of USS is firstly carried out. Then, the optimal trajectories are planning according to the task assignment result and the swarm individuals are driven to the temporary target state. At the next moment, the tasks are reassigned again according to the current location of the swarm individuals. The above steps are repeated until all swarm individuals reach the desired target position.

3.2 Sinkhorn-Newton for Entropic Optimal Transport

According to [33], The solution to (13) is unique and has the matrix form

$$\forall (i, j) \in [\![N]\!] \times [\![N]\!], \boldsymbol{P}^* = diag(\boldsymbol{\alpha})\boldsymbol{K}diag(\boldsymbol{\beta}), p_{i,j} = \alpha_i K_{i,j} \beta_j \tag{14}$$

where $\boldsymbol{K} = \exp(-\boldsymbol{c}^i_{N_h}(\boldsymbol{x}_i, \boldsymbol{x}^d_j)/\varepsilon)$, $K_{i,j}$ is the element of matrix $\boldsymbol{K}$, α_i is the ith element of $\boldsymbol{\alpha} \in \mathbb{R}^{1\times N}$, and β_j is the jth element of $\boldsymbol{\beta} \in \mathbb{R}^{1\times N}$.

To reduce the computational burden, the Sinkhorn-Newton method is proposed to solve $\boldsymbol{P}^*$. It is seen in (14) that the solution $\boldsymbol{P}^*$ is a mapping of $\boldsymbol{K}$ through $\boldsymbol{\alpha}$ and $\boldsymbol{\beta}$. Given $\boldsymbol{K}$, $\boldsymbol{P}^*$ can be computed by solving mappings $\boldsymbol{\alpha}$ and $\boldsymbol{\beta}$ iteratively. From the mass conservation condition of optimal transport, it inferred that $\boldsymbol{\mu}_a$, $\boldsymbol{\nu}_b$ and $\boldsymbol{\alpha}$, $\boldsymbol{\beta}$ are satisfied

$$\begin{cases} diag(\boldsymbol{\alpha})\boldsymbol{K}diag(\boldsymbol{\beta})\boldsymbol{1}_N = \boldsymbol{\mu}_a \\ diag(\boldsymbol{\beta})\boldsymbol{K}^{\mathrm{T}}diag(\boldsymbol{\alpha})\boldsymbol{1}_N = \boldsymbol{\nu}_b \end{cases} \tag{15}$$

then it follows that

$$\begin{cases} diag(\boldsymbol{\alpha})(\boldsymbol{K}\boldsymbol{\beta}) = \boldsymbol{\mu}_a \\ diag(\boldsymbol{\beta})(\boldsymbol{K}^{\mathrm{T}}\boldsymbol{\alpha}) = \boldsymbol{\nu}_b \end{cases} \tag{16}$$

According to Newton's method, the Sinkhorn-Newton method is designed, and the Newton iteration is derived to find a root of the function

$$\boldsymbol{G}(\boldsymbol{\alpha}, \boldsymbol{\beta}) = \begin{bmatrix} diag(\boldsymbol{\alpha})\boldsymbol{K}\boldsymbol{\beta} - \boldsymbol{\mu}_x \\ diag(\boldsymbol{\beta})\boldsymbol{K}^{\mathrm{T}}\boldsymbol{\alpha} - \boldsymbol{\nu}_y \end{bmatrix} \tag{17}$$

and the Jacobian matrix is

$$\boldsymbol{J_G}(\boldsymbol{\alpha}, \boldsymbol{\beta}) = \begin{bmatrix} diag(\boldsymbol{K}\boldsymbol{\beta}) & diag(\boldsymbol{\alpha})\boldsymbol{K} \\ diag(\boldsymbol{\beta})\boldsymbol{K}^{\mathrm{T}} & diag(\boldsymbol{K}^{\mathrm{T}}\boldsymbol{\alpha}) \end{bmatrix} \tag{18}$$

Then the Newton iteration for Eq. (16) is given by

$$\begin{bmatrix} \boldsymbol{\alpha}^{k+1} \\ \boldsymbol{\beta}^{k+1} \end{bmatrix} = \begin{bmatrix} \boldsymbol{\alpha}^{k} \\ \boldsymbol{\beta}^{k} \end{bmatrix} - \boldsymbol{J_G}(\boldsymbol{\alpha}^k, \boldsymbol{\beta}^k)^{-1} \boldsymbol{G}(\boldsymbol{\alpha}^k, \boldsymbol{\beta}^k) \tag{19}$$

By several iterations, the optimal mapping $\boldsymbol{\alpha}^*$, $\boldsymbol{\beta}^*$ is obtained when the cutoff condition is satisfied. Hence, the optimal solution is

$$\boldsymbol{P}^* = diag(\boldsymbol{\alpha}^*)\boldsymbol{K}diag(\boldsymbol{\beta}^*) \tag{20}$$

Note that the initial values $\boldsymbol{\alpha}^0$ and $\boldsymbol{\beta}^0$ is arbitrary.

4 Application to Unmanned Surface Vehicle Swarm

In this section, the proposed simultaneous task assignment and trajectory planning method is applied to unmanned surface vehicle (USV) swarm. According to Eqs. (8), (12) and (13), the motion state $\boldsymbol{x}_i$ of USV and the cost function $\mathcal{L}_i(\boldsymbol{x}_i(k), \boldsymbol{u}_i(k); \boldsymbol{x}_j^d)$ of MPC need to be given.

4.1 The Mathematical Modeling of USV Swarm

Assuming that only planar maneuvers are considered. Hence, the surge, sway, and yaw motions are investigated, while the roll, pitch, and heave motions of the USV need not be studied. Hence, the kinematic model of USV with three degrees of freedom is defined as [35]

$$\dot{\boldsymbol{\eta}}_i = \boldsymbol{R}(\varphi_i)\boldsymbol{v}_i \tag{21}$$

where

$$\boldsymbol{R}(\varphi_i) = \begin{bmatrix} \cos\varphi_i & -\sin\varphi_i & 0 \\ \sin\varphi_i & \cos\varphi_i & 0 \\ 0 & 0 & 1 \end{bmatrix}, \boldsymbol{\eta}_i = (x_i, y_i, \varphi_i)^{\mathrm{T}}, \boldsymbol{v}_i = (u_i, v_i, r_i)^{\mathrm{T}} \tag{22}$$

where $\boldsymbol{R}(\varphi_i)$ is rotation matrix, x_i, y_i and φ_i denote the position and orientation of the i-th USV in inertial frame, $i = 1, \ldots, N$. u_i, v_i, r_i represent the ith USV's velocities of surge, sway, and yaw in body frame, respectively. The relationship between the inertial frame and body frame is shown in Fig. 1. Let $F_E\{O_E X_E Y_E\}$ be an inertial frame, which is centered on the relative stationary reference, with the X_E-axis pointing due north and the Y_E-axis pointing due east. $F_B\{O_B X_B Y_B\}$ be the body frame fixed to the center of mass of USV, where the positive direction of the X_B-axis and Y_B-axis correspond to the rightward and forward directions of the USV, respectively.

The dynamic model of the USV is defined as follows [35, 36]

$$\begin{aligned} \dot{u}_i &= \kappa_1 u_i + \kappa_2 \tau_i \\ \dot{r}_i &= \kappa_3 r_i + \kappa_4 \zeta_i \end{aligned} \tag{23}$$

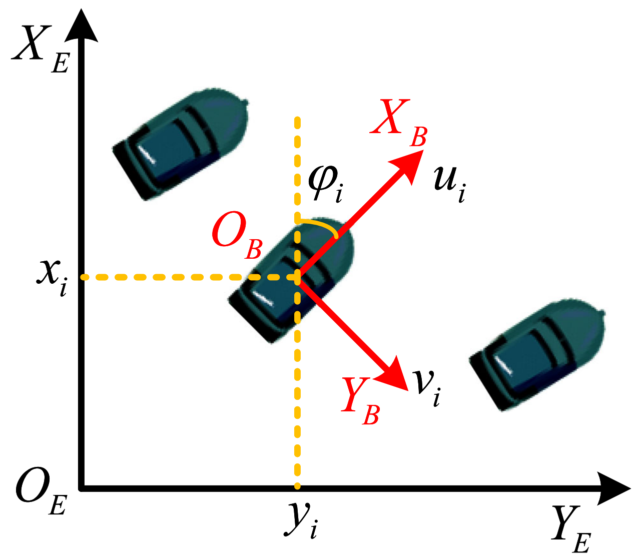

Fig. 1 The definition of reference coordinate system

where $\dot{u}_i$ and $\dot{r}_i$ indicate the forward and yaw accelerations of the i-th USV, respectively. τ and ζ denote the thrust and rudder of the i-th USV, respectively. κ_1, κ_2, κ_3, and κ_4 are the model parameters.

Let $\boldsymbol{x}_i(k) = [x_i(k), y_i(k), \psi_i(k), u_i(k), v_i(k), r_i(k)]^{\mathrm{T}}$ denote the state at time step k, $\boldsymbol{u}_i(k) = [\tau_i(k), \zeta_i(k)]^{\mathrm{T}}$ indicate the control input at time step k. The linearized state space model is described as

$$\tilde{\boldsymbol{x}}_i(k+1) = \boldsymbol{A}_i(k)\tilde{\boldsymbol{x}}_i(k) + \boldsymbol{B}_i(k)\tilde{\boldsymbol{u}}_i(k) \tag{24}$$

$$\boldsymbol{A}_i(k) = \boldsymbol{I}_{6\times6} + \begin{bmatrix} 0 & 0 & -u_i\sin\varphi_i - v_i\cos\varphi_i & \cos\varphi_i & -\sin\varphi_i & 0 \\ 0 & 0 & u_i\cos\varphi_i - v_i\sin\varphi_i & \sin\varphi_i & \cos\varphi_i & 0 \\ 0 & 0 & 0 & 0 & 0 & 1 \\ 0 & 0 & 0 & \kappa_1 & 0 & 0 \\ 0 & 0 & 0 & 0 & 0 & 0 \\ 0 & 0 & 0 & 0 & 0 & \kappa_3 \end{bmatrix} \cdot dt \tag{25}$$

$$\boldsymbol{B}_i(k) = \begin{bmatrix} 0 & 0 & 0 & \kappa_2 & 0 & 0 \\ 0 & 0 & 0 & 0 & 0 & \kappa_4 \end{bmatrix}^{\mathrm{T}} \cdot dt \tag{26}$$

where $\tilde{\boldsymbol{x}}_i = \boldsymbol{x}_i - \boldsymbol{x}_i(0)$, $\tilde{\boldsymbol{u}}_i = \boldsymbol{u}_i - \boldsymbol{u}_i(0)$. $\boldsymbol{x}_i^0$ and $\boldsymbol{u}_i^0$ are the state and control input at $k = 0$, respectively. dt is discretization step.

4.2 The Cost Function Design for MPC

In this subsection, the cost function is designed as $\mathcal{L}_i(\boldsymbol{x}_i(k), \boldsymbol{u}_i(k); \boldsymbol{x}_j^d) = J_{N_h}(\boldsymbol{x}_i, \boldsymbol{u}_i, k) + J_{ao}(\boldsymbol{x}_i, k)$. $J_{N_h}(\boldsymbol{x}_i, \boldsymbol{u}_i, k)$ is the cost of state and control input, and $J_{ao}(\boldsymbol{x}_i, k)$ is the cost of obstacle avoidance.

Fig. 2 The diagram of obstacle avoidance

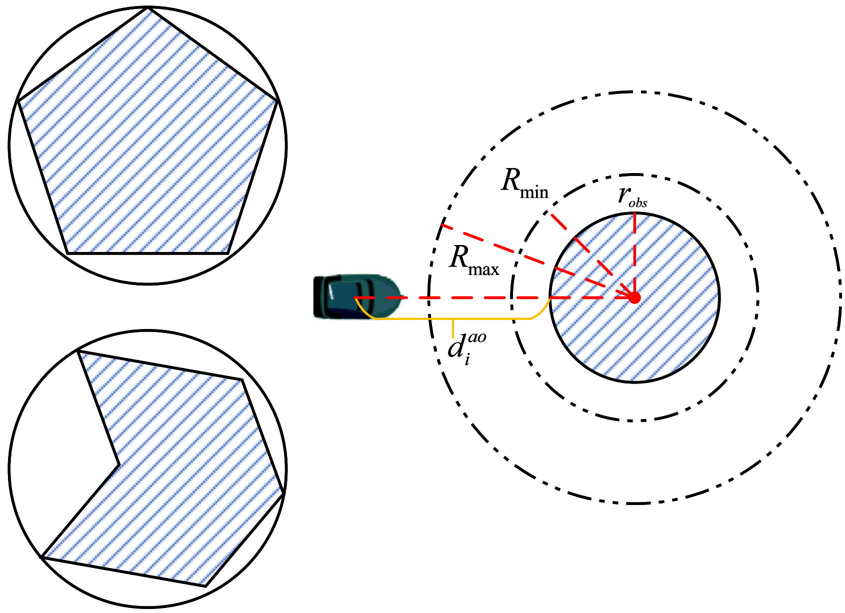

The cost function considering the state and control input is defined as

$$\begin{aligned} J_{N_h}(\boldsymbol{x}_i, \boldsymbol{u}_i, k) = & \sum_{p=1}^{N_h-1} (||\boldsymbol{x}_i(k+p|k) - \boldsymbol{x}_j^d||_{\boldsymbol{Q}}^2 \\ & + ||\boldsymbol{u}_i(k+p|k) - \boldsymbol{u}_j^d||_{\boldsymbol{R}}^2) \\ & + ||\boldsymbol{x}_i(k+N_h|k) - \boldsymbol{x}_j^d||_{\boldsymbol{Q}_{N_h}}^2 \end{aligned} \tag{27}$$

where $\boldsymbol{Q}$, $\boldsymbol{R}$, $\boldsymbol{Q}_{N_h}$ are positive-definite weight matrices for state, control input and terminal state respectively. The cost function of terminal state is utilized to ensure the stability of the model predictive controller.

In this paper, a collision avoidance cost function is introduced to prevent collisions. Prior to this, the obstacle is modeled and the collision avoidance mechanisms is investigated. To simplify the modeling complexity, a circular envelope is used to enclose the obstacles. The diameter of the envelope circle is determined as the longest distance across the obstacle, with its midpoint denoted as (x_{obs}, y_{obs}), and the radius denoted as r_{obs}.

It is seen in Fig. 2 that the area surrounding an obstacle is divided into three zones by utilizing the distance between the USV and the obstacle, including the safety zone, obstacle avoidance zone, and danger zone. $R_{\max}$ and $R_{\min}$ denote the radius of the obstacle avoidance zone and the danger zone, respectively. d_i^{ao} indicates the shortest distance between the

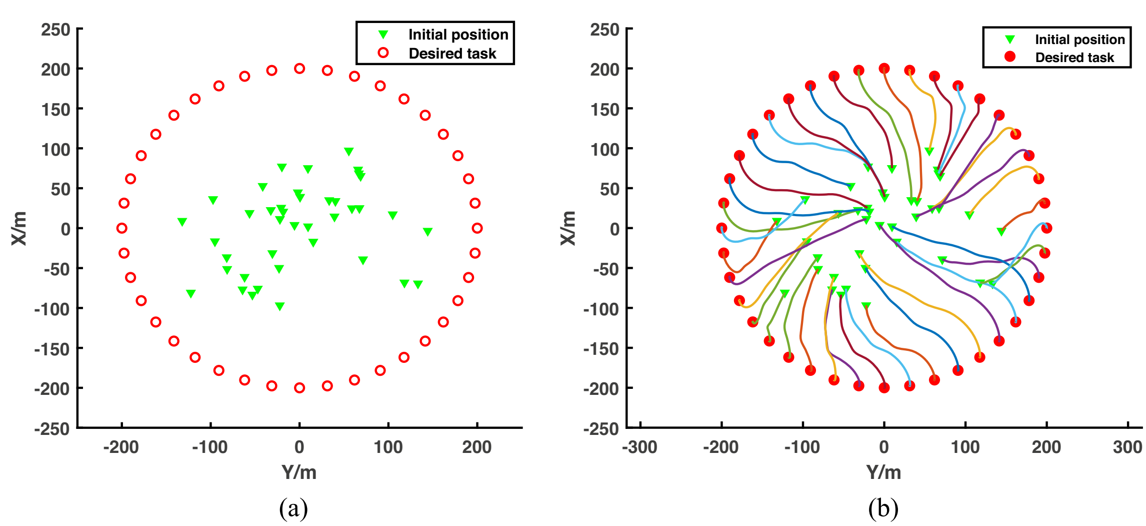

Fig. 3 The result of simultaneous task assignment and trajectory planning for USV swarm without obstacle

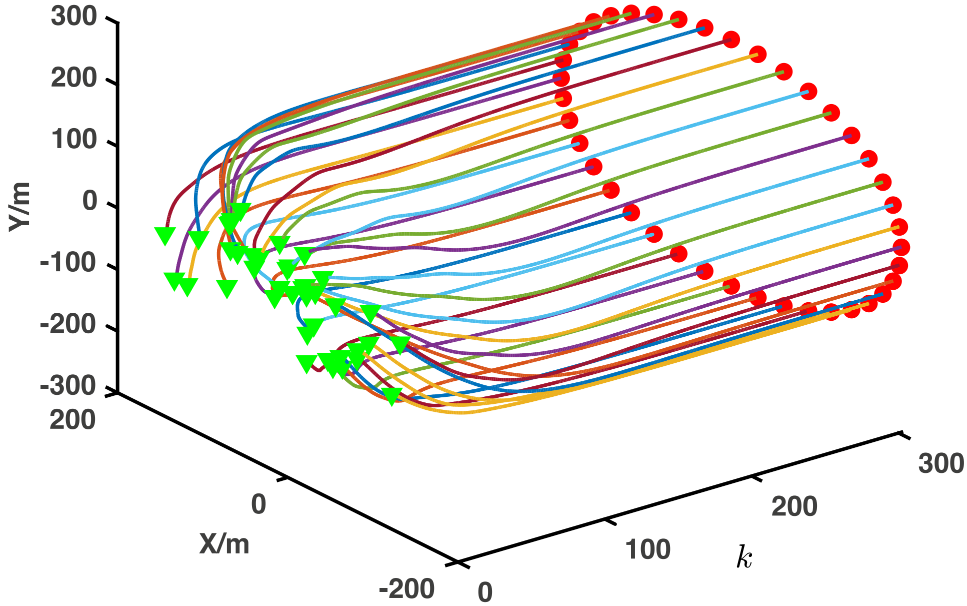

Fig. 4 The trajectories of USV swarm over time step k

USV and the obstacle. If $d_i^{ao} > R_{\max} - r_{obs}$, the trajectory tracking mode is engaged. If $R_{\min} - r_{obs} \leq d_i^{ao} \leq R_{\max} - r_{obs}$, the collision avoidance mode is activated. If $d_i^{ao} < R_{\min} - r_{obs}$, the USV is considered to be too close to the obstacle, resulting in a failure to avoid the obstacle.

Hence, the cost function of obstacle avoidance for the ith USV at time k is defined as

$$J_{ao}(\boldsymbol{x}_i, k) = \begin{cases} 0, if\ d_i^{uo}(k) \geqslant R_{\max} \\ \sum_{p=1}^{N_h} -\lambda(d_i^{ao}(k+p|k) - (R_{\min} - r_{obs})), if\ R_{\min} \leqslant d_i^{uo}(k) < R_{\max} \\ \infty, if\ d_i^{uo}(k) < R_{\min} \end{cases} \tag{28}$$

where $d_i^{uo}(k) = d_i^{ao}(k) + r_{obs}$, λ is penalty parameter, and

$$d_i^{ao}(k) = \sqrt{(x_i(k) - x_{obs})^2 + (y_i(k) - y_{obs})^2} - r_{obs} \tag{29}$$

$$d_i^{ao}(k+p|k) = \sqrt{(x_i(k+p|k) - x_{obs})^2 + (y_i(k+p|k) - y_{obs})^2} - r_{obs} \tag{30}$$

5 Simulation and Experimental Verification

In this section, the effectiveness of the designed simultaneous task assignment and trajectory planning scheme is verified

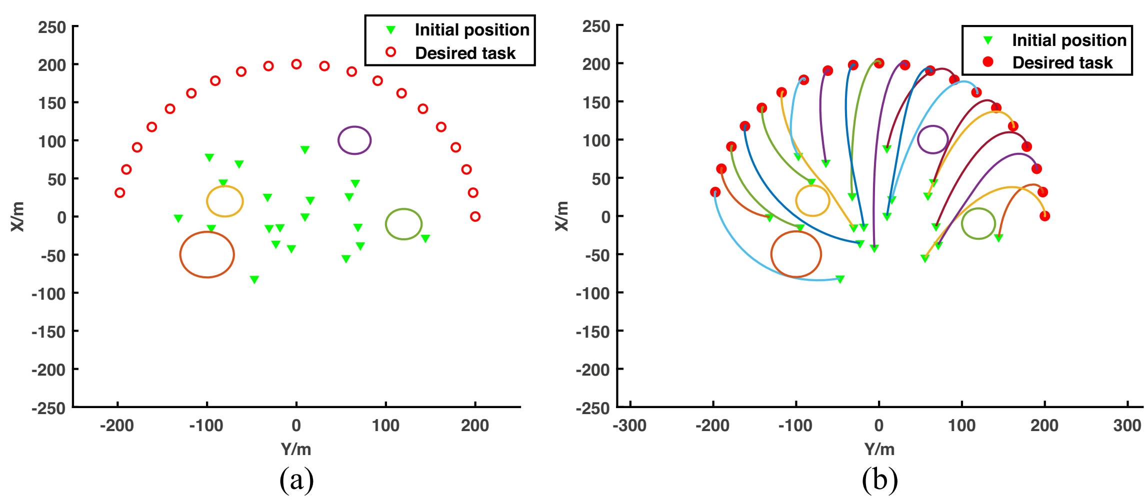

Fig. 5 The result of simultaneous task assignment and trajectory planning for USV swarm with obstacles

Table 1 Comparison of computation time and completion time for three algorithms

Task number/N	OT-MPC		PSO		Ant Colony	
	T_c (s)	T_f (s)	T_c (s)	T_f (s)	T_c (s)	T_f (s)
10	0.00359	17.96848	0.00602	30.77694	0.00586	29.33018
50	0.00956	155.25466	1.15527	233.96935	1.13426	229.60527
100	0.03926	1010.61458	9.82803	1802.97535	8.02310	1635.12642

with the USV swarm by numerical simulations and experimental tests.

5.1 Simulation Results

According to the dynamic model (23), the unknown parameters need to be obtained through model identification experiments. The Zigzag experiment and Rotation experiment [37] are designed to identify the USV's model parameters. According to the collected experimental data, the parameters are calculated by least square method. Hence, the USV model parameters are $\kappa_1 = -1.6812$, $\kappa_2 = 3.6594$, $\kappa_3 = -3.1772$ and $\kappa_4 = 4.9305$. The model discretization step $dt = 0.02$. The task space is in area $[-250, 250]$m $\times$ $[-250, 250]$m. Moreover, the following three cases are simulated.

Case #1: No obstacles are set in the simulation scenario. The number of USVs $N = 40$. It is observed in Fig. 3(a) that the initial position of the USV swarm is a uniform random distribution, and the desired tasks are evenly distributed on a circle with a radius of 200m. The initial velocities of USVs are zero and the initial heading angles are random. When implementing the developed simultaneous task assignment and trajectory planning algorithm, the related parameters are chosen as $N_h = 50$, $\varepsilon = 2.5$, $\boldsymbol{\alpha}^0 = \boldsymbol{\beta}^0 = \mathbf{1}_N$. $\boldsymbol{Q} = 1 \times 10^{-2} * \boldsymbol{I}_{6\times6}$, $\boldsymbol{R} = 1 * \boldsymbol{I}_{2\times2}$, and $\boldsymbol{Q}_{N_h} = 5 \times 10^{-2} * \boldsymbol{I}_{6\times6}$. Note that without affecting the dynamic processing of the swarm system, the prediction time step N_h is as small as possible. The selection of $\boldsymbol{Q}$, $\boldsymbol{R}$ and $\boldsymbol{Q}_{N_h}$ need to be based on different requirements for system performance. $\varepsilon > 0$ is selected by trial and error method.

When the simultaneous task assignment and trajectory planning algorithm is implemented in this case, the task assignment result is illustrated in Fig. 3(b). The proposed method assigns optimal tasks to each swarm individual and generates collision-conflict free trajectories. It is further verified in Fig. 4 that the proposed method generates collision-free time series trajectories.

Case #2: Obstacles are set in the simulation scenario. The number of USVs $N = 20$. It is seen in Fig. 5(a) that the initial position of the USV swarm is a uniform random distribution, and the desired tasks are evenly distributed on a semicircular pattern resembling an expulsion formation. Additionally, the obstacles are located at coordinates (10, 5), (8, 2), (65, 10), and (12, 10). The initial velocities of USVs are zero and the initial heading angles are random. The value of ε is set to 1.2, while other parameters are kept same with the Case #1. Figure 5(b) illustrates that each USV in the swarm is successfully assigned to its corresponding task and avoiding all obstacles to reach the positions of desired tasks.

Case #3: Simulations on analyzing computation time and completion time. The simulations were done on computer with Intel Core i7-9750H CPU @2.6GHZ and 16GB RAM. To verify the superiority of the proposed method in terms of computational efficiency, PSO algorithm and Ant Colony algorithm are used for comparison. Table 1 shows the computation time and completion time of three algorithm. T_c denotes the computation time and T_f denotes the completion time. Even for a scenario with 100 USVs and 100 tasks, the computation time of the proposed method is still well under 0.1 second. Compared to other two methods, the method proposed in this paper can better demonstrate the advantages of global optimization as the swarm size increases.

To further illustrate the reliability of the results, The mean value and standard deviation of computation time and com-

Table 2 The mean value and standard deviation of computation time and completion time for task assignment

Task number/N	Computation time		Completion time	
	T_c (s)	σ_{T_c} (s)	T_f (s)	σ_{T_f} (s)
10	0.00360	0.0005	18.90049	0.36206
50	0.00955	0.0030	153.58283	1.54302
100	0.03928	0.0051	1006.16914	2.63427

Fig. 6 The environment of outdoor experiment

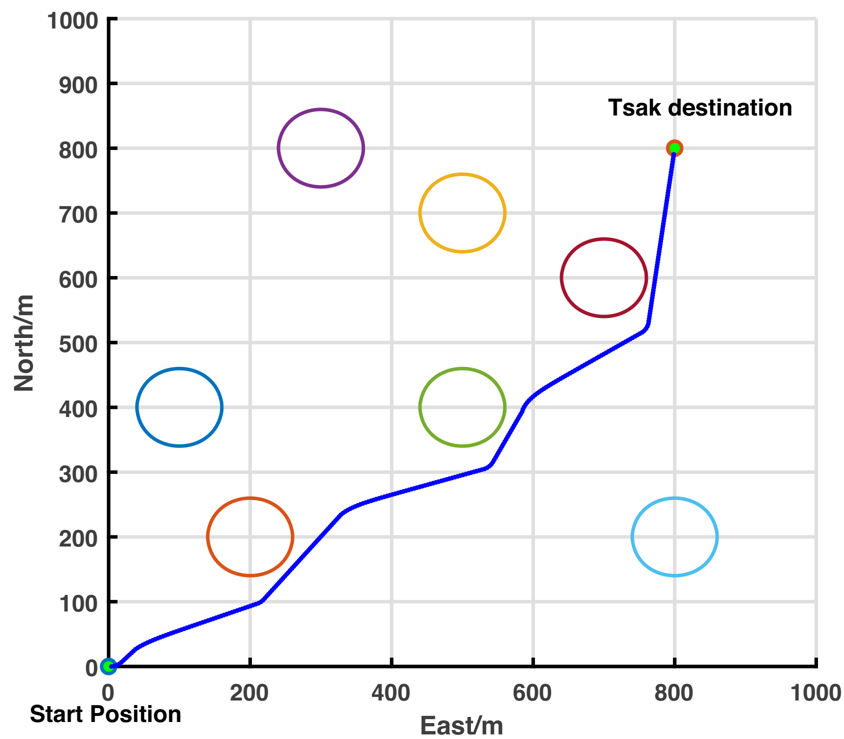

Fig. 7 The experiment result: The simultaneous task assignment and trajectory planning for single USV

pletion time for task assignment are displayed in Table 2. The mean value and standard deviation are obtained through running 50 Monte Carlo simulation. For the scenario with 100 USVs and 100 tasks, the mean value and standard deviation of computation time are 0.03928s and 0.0051s, respectively. Correspondingly, the completion times are 1006.16914s and 2.63427s, respectively. The fact that the standard deviation differs by several orders of magnitude from the real data suggests that the proposed algorithm is relatively stable.

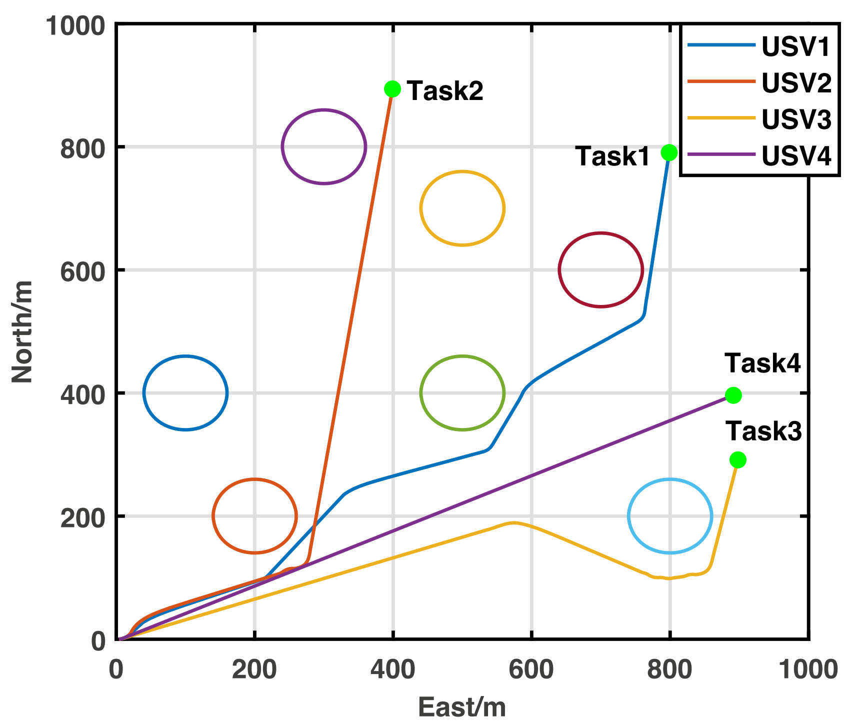

Fig. 8 The experiment result: The simultaneous task assignment and trajectory planning for four USVs (One real and three virtual)

5.2 Experimental Verification

In this section, an outdoor experiment is conducted using the catamaran unmanned ship provided by Harbin Institute of Technology, Weihai, as shown in Fig. 6. The USV has dimensions of 11.98m in length, 5.65m in width, and 1.53m in depth. It is equipped with various advanced technologies, including radar, photoelectric pod, AD hoc base station, and inertial navigation equipment, capable of providing accurate navigation information. The USV offers three operational modes: manual driving, remote control, and autonomous navigation, providing flexibility for conducting experiments and evaluating performance. To overcome limitations on the number of real USV and to ensure safety, the experimental was set up into two scenarios.

Scenario #1: A single USV was utilized to perform simultaneous task assignment and obstacle avoidance trajectory planning.

The experiment was designed in an open sea area with an approximate size of 1000 m^2. The starting point of the USV was set as $(0, 0)$, and the task point was chosen as $(800, 800)$. To create a challenging environment, the obstacles was placed in a plurality of locations, including $(400, 100)$, $(200, 200)$, $(700, 500)$, $(800, 300)$, $(400, 500)$, $(200, 800)$, and $(600, 700)$. The USV was set to operate in autonomous navigation mode. By analyzing the navigation data, it was observed in Fig. 7 that the USV successfully navigated to the task point without any collisions.

Scenario #2: A virtual-real combination experiment was designed, and the virtual-real combination system includes a real USV and three virtual USVs generated by the ground station. This approach allows for the simulation of larger swarms of USV while ensuring safety, and validates the effectiveness of simultaneous task assignment and trajectory planning methods for USS.

The experimental scenario was set up as in Scenario #1. Real-time data from the physical USV and simulation data from the ground station were exchanged through wireless communication. The experimental results in Fig. 8 demonstrate that the successful task assignment and trajectory planning for each of the four USVs. Each USV was assigned a single task and navigated to the corresponding task position without any collisions. It is worth mentioning that although there may be instances of overlapping and crossing of USV swarm trajectories, these trajectories occur at different time and do not lead to collisions.

6 Conclusions

The simultaneous task assignment and trajectory planning problem of the unmanned swarm system was addressed. A unified cost function by coupling the task assignment and trajectory planning sub-problems together by using optimal transport and model predictive control. The optimal transport method is utilized to match tasks randomly to unmanned system vehicles based on their costs, while the model predictive control is employed to iteratively optimize the trajectories of the unmanned system vehicles based on real-time feedback and predictions. Each solution of the cost function requires the mutual coordination of task assignment and path planning. Another feature of this approach was that it is capable of rapidly obtaining the global optimal solution and demonstrates high efficiency and scalability for large-scale USS tasks by using the Sinkhorn-Newton algorithm.

Although the proposed method can solve both task assignment and trajectory planning problems of large-scale swarm simultaneously, only the one-to-one task assignment was investigated. Future research works lie in exploring further optimizations and extensions of the proposed method for different scenarios and applications, especially scenarios where the number of swarm individuals and tasks are not same. Moreover, the idea of prescribed time [38] should be introduced to investigate the assignment of tasks at a specific time.

Author Contributions All authors contributed to the study conception and design. Method designing, coding, experiment preparation, data collection and analysis were performed by Xiwei Wu. The first draft of the manuscript was written by Xiwei Wu and Bing Xiao, and all authors commented on previous versions of the manuscript. All authors read and approved the final manuscript.

Funding This work was supported by the National Natural Science Foundation of China (No. 11972373), the Natural Science Foundation of Shandong Province (No. ZR2020ME265, ZR2021ME155), the Innovation Capability Improvement Project for Technology Oriented Small and Medium-sized Enterprises of Shandong Province (No. 2021TSGC1376), the Key Research and Development Program of Shandong (No. 2022ZLGX04).

Declarations

Competing of interest The authors have no relevant financial or non-financial interests to disclose.

Consent to publish The authors gave their authorization for the publishing of this article.

References

1. Liu, Z., Zhang, Y., Yu, X., Yuan, C.: Unmanned surface vehicles: An overview of developments and challenges. Annu. Rev. Control. **41**, 71–93 (2016)
2. Tahir, A., Böling, J., Haghbayan, M.-H., Toivonen, H.T., Plosila, J.: Swarms of unmanned aerial vehicles-a survey. J. Ind. Inf. Integr. **16**, 100106 (2019)
3. Gong, X., Wang, T., Huang, T., Cui, Y.: Toward safe and efficient human–swarm collaboration: A hierarchical multi-agent pickup and delivery framework. IEEE Trans. Intell. Veh. **8**(2), 1664–1675 (2022)
4. Zhen, Z., Chen, Y., Wen, L., Han, B.: An intelligent cooperative mission planning scheme of uav swarm in uncertain dynamic environment. Aerosp. Sci. Technol. **100**, 105826 (2020)
5. Qin, Z., Lin, Z., Yang, D., Li, P.: A task-based hierarchical control strategy for autonomous motion of an unmanned surface vehicle swarm. Appl. Ocean Res. **65**, 251–261 (2017)
6. Cao, L., Xiao, B., Golestani, M., Ran, D.: Faster fixed-time control of flexible spacecraft attitude stabilization. IEEE Trans. Ind. Inform. **16**(2), 1281–1290 (2020)
7. Wu, X., Xiao, B., Cao, L., Hu, X.: Robust macroscopic density control of microsatellite swarm via local measurement. IEEE Transactions on Aerospace and Electronic Systems, pp. 1–14. https://doi.org/10.1109/TAES.2023.3326109 (2023)
8. Giles, K., Giammarco, K.: A mission-based architecture for swarm unmanned systems. Syst. Eng. **22**(3), 271–281 (2019)
9. An, D., Mu, Y., Wang, Y., Li, B., Wei, Y.: Intelligent path planning technologies of underwater vehicles: a review. J. Intell. Robot. Syst. **107**(2), 22 (2023)
10. Wang, Z., Zhang, J.: A task allocation algorithm for a swarm of unmanned aerial vehicles based on bionic wolf pack method. Knowl.-Based Syst. **250**, 109072 (2022)
11. Xue, K., Huang, Z., Wang, P., Xu, Z.: An exact algorithm for task allocation of multiple unmanned surface vehicles with minimum task time. J. Mar. Sci. Eng. **9**(8), 907 (2021)
12. Ho, S.-Y., Lin, H.-S., Liauh, W.-H., Ho, S.-J.: Opso: Orthogonal particle swarm optimization and its application to task assignment problems. IEEE Trans. Syst. Man Cybern.-Part A: Syst. Hum. **38**(2), 288–298 (2008)
13. Yi, X., Zhu, A., Yang, S.X., Luo, C.: A bio-inspired approach to task assignment of swarm robots in 3-d dynamic environments. IEEE Trans. Cybern. **47**(4), 974–983 (2016)
14. Xia, G., Sun, X., Xia, X.: Multiple task assignment and path planning of a multiple unmanned surface vehicles system based on improved self-organizing mapping and improved genetic algorithm. J. Mar. Sci. Eng. **9**(6), 556 (2021)
15. Tang, Z., Gong, M., Xie, Y., Li, H., Qin, A.K.: Multi-task particle swarm optimization with dynamic neighbor and level-based intertask learning. IEEE Trans. Emerg. Top. Comput. Intell. **6**(2), 300–314 (2021)
16. Ma, S., Guo, W., Song, R., Liu, Y.: Unsupervised learning based coordinated multi-task allocation for unmanned surface vehicles. Neurocomputing **420**, 227–245 (2021)
17. Roberge, V., Tarbouchi, M., Labonté, G.: Comparison of parallel genetic algorithm and particle swarm optimization for real-time uav path planning. IEEE Trans. Ind. Inform. **9**(1), 132–141 (2012)
18. Girija, S., Joshi, A.: Fast hybrid pso-apf algorithm for path planning in obstacle rich environment. IFAC-PapersOnLine **52**(29), 25–30 (2019)
19. Bibuli, M., Singh, Y., Sharma, S., Sutton, R., Hatton, D., Khan, A.: A two layered optimal approach towards cooperative motion planning of unmanned surface vehicles in a constrained maritime environment. IFAC-PapersOnLine **51**(29), 378–383 (2018)
20. Li, D., Li, Y., Liu, X., Yang, B., Huang, X., Yang, Y., Wang, B., Li, S.: Pseudospectral convex programming for free-floating space manipulator path planning. Space: Sci & Technol **3**, 0030 (2023)
21. Wu, X., Xiao, B., Wu, C., Guo, Y.: Centroidal voronoi tessellation and model predictive control–based macro-micro trajectory optimization of microsatellite swarm. Space: Science & Technology **2022** (2022)
22. Zhao, Z., Zhu, B., Zhou, Y., Yao, P., Yu, J.: Cooperative path planning of multiple unmanned surface vehicles for search and coverage task. Drones **7**(1), 21 (2023)
23. Eun, Y., Bang, H.: Cooperative task assignment/path planning of multiple unmanned aerial vehicles using genetic algorithm. J. Aircr. **46**(1), 338–343 (2009)
24. Schillinger, P., Bürger, M., Dimarogonas, D.V.: Simultaneous task allocation and planning for temporal logic goals in heterogeneous multi-robot systems. Int. J. Rob. Res. **37**(7), 818–838 (2018)
25. An, S., Kim, H.J.: Simultaneous task assignment and path planning using mixed-integer linear programming and potential field method. In: 2013 13th International conference on control, automation and systems (ICCAS 2013), pp. 1845–1848 (2013). IEEE
26. Turpin, M., Michael, N., Kumar, V.: Trajectory planning and assignment in multirobot systems. In: Algorithmic foundations of robotics X: proceedings of the tenth workshop on the algorithmic foundations of robotics, pp. 175–190 (2013). Springer
27. Turpin, M., Michael, N., Kumar, V.: Capt: Concurrent assignment and planning of trajectories for multiple robots. Int. J. Rob. Res. **33**(1), 98–112 (2014)
28. Yang, F., Chakraborty, N.: Chance constrained simultaneous path planning and task assignment for multiple robots with stochastic path costs. In: 2020 IEEE international conference on robotics and automation (ICRA), pp. 6661–6667 (2020). IEEE
29. Liu, Z., Wei, H., Wang, H., Li, H., Wang, H.: Integrated task allocation and path coordination for large-scale robot networks with uncertainties. IEEE Trans. Autom. Sci. Eng. **19**(4), 2750–2761 (2021)
30. Peyré, G., Cuturi, M., et al.: Computational optimal transport: With applications to data science. Foundations and Trends® in Machine Learning **11**(5-6), 355–607 (2019)
31. Cuturi, M.: Sinkhorn distances: Lightspeed computation of optimal transport. Advances in Neural Information Processing Systems **26** (2013)
32. Solomon, J.: Optimal transport on discrete domains. AMS Short Course on Discrete Differential Geometry (2018)
33. Peyré, G., Cuturi, M., et al.: Computational optimal transport. Center for Research in Economics and Statistics Working Papers, pp. 2017–86 (2017)
34. Ito, K., Kashima, K.: Entropic model predictive optimal transport over dynamical systems. Automatica **152**, 110980 (2023)
35. Sonnenburg, C.R., Woolsey, C.A.: Modeling, identification, and control of an unmanned surface vehicle. J. Field Robot. **30**(3), 371–398 (2013)
36. Mu, D., Wang, G., Fan, Y., Sun, X., Qiu, B.: Modeling and identification for vector propulsion of an unmanned surface vehicle: Three degrees of freedom model and response model. Sensors **18**(6), 1889 (2018)
37. Zhang, M., He, Y., Xiong, J.: Research on the unmanned surface vehicle kinetics model for automatic berthing. In: Advances in guidance, navigation and control: proceedings of 2020 international conference on guidance, navigation and control, ICGNC 2020, Tianjin, China, October 23–25, 2020, pp. 3659–3670 (2022). Springer

38. Xiao, B., Wu, X., Cao, L., Hu, X.: Prescribed time attitude tracking control of spacecraft with arbitrary disturbance. IEEE Trans. Aerosp. Electron. Syst. **58**(3), 2531–2540 (2022)

Publisher's Note Springer Nature remains neutral with regard to jurisdictional claims in published maps and institutional affiliations.

Xiwei Wu received the B.S. degree in automation from Nanjing Normal University, Nanjing, China, in 2017, and the M.S. degree in control engineering from Northwestern Polytechnical University, Xi'an, China, in 2020. Since 2020, he has been working toward the Ph.D. degree in control science and engineering with the School of Automation, Northwestern Polytechnical University, Xi'an, China. His current research interests include navigation, guidance, and control of swarm microsatellites.

Bing Xiao received the B.S. degree in mathematics from Tianjin Polytechnic University, Tianjin, China, in 2007, and the M.S. and Ph.D. degrees in control science and engineering from Harbin Institute of Technology, Harbin, China, in 2010 and 2014, respectively. He is currently a Professor with the School of Automation, Northwestern Polytechnical University. His research interests include aircraft control, advanced control design, and its application to unmanned aerial vehicles.

Lu Cao received the B.S., M.S., and Ph.D. degrees in navigation and control of spacecraft from the National University of Defense Technology, Changsha, China, in 2007, 2010, and 2014, respectively. He was with the McGill University as a Visiting Ph.D. student from 2013 to 2014 and focused on the dynamics, navigation, and control of spacecraft. He is currently a Research Fellow with the National Innovation Institute of Defense Technology, Chinese Academy of Military Sciences, Beijing, China. He has more than ten years experiences in the nano-satellite engineering. His research interests include the areas of satellite navigation, control and dynamics, and estimation theory research.

Haibin Huang received his Bachelor's degree in Automation from Qingdao University of Science and Technology in 2005, his Master's degree in Control Science and Engineering from Harbin Institute of Technology in 2007, and his Ph.D. degree in Control Science and Engineering from Harbin Institute of Technology in 2011. He is currently an Associate Professor in the Department of Control Science and Engineering at Harbin Institute of Technology. His main research interests include intelligent autonomous control of unmanned systems, cross-domain cooperative control of unmanned systems, and game-theoretic analysis of unmanned systems cluster defense and attack.